Structured Noise Analysis in Intrinsic Optical Imaging

Haibing Yin, Yadong Liu, Zongtan Zhou, Ming Li, Yucheng Wang, Dewen Hu*
Department of Automatic Control, College of Mechatronics and Automation
National University of Defense Technology,
Changsha, Hunan 410073, PRC
*Corresponding author: dwhu@nudt.edu.cn

***Abstract*—In this paper, a novel structured noises-reduction technique for OI data is proposed. Canonical correlation analysis (CCA) technique is exploited to separate the underlying independent sources among which the neural response signal is picked out by the correlation analysis. The white noise (WN) criterion is applied to discern the structured components from the unstructured ones. The energy of structured noises is then eliminated from the original data. Monte Carlo simulation is used to test the validity of the procedure. The result shows that after the noise reduction, the true positive rate improves significantly without raising the false positive rate. Five sets of OI data of single trial collected from the HP area of rat's cortex are processed by the procedure and the resulting activation maps present more detailed spatial architecture than those without noise reduction.**

Keywords—Optical Image (OI), Canonical Correlation Analysis(CCA), Monte Carlo simulation

I. INTRODUCTION

Intrinsic Optical Imaging (OI) is relatively a new functional brain imaging technique first appeared in 1980's [8] and from then on the number of studies using it has been growing rapidly [3]. Functional physiological changes, such as increases in the blood volume, hemoglobin oxymetry changes, and light scattering changes, result in intrinsic tissue reflectance changes that are exploited in OI to map functional brain activity. The technique offers high spatio-temporal resolution and is relatively noninvasive, and so has the opportunity to image development and plasticity of neuron in a long duration [3].

Without deliberate neuronal activity of the brain cortex, the OI signal is a stochastic sum of various physiological and artifact related signal sources. These sources include the respiration/pulse-induced vasomotion, the subject movements, light source instability, shot noises and other complicated image artifacts. The superposition of these noise sources on the neural response signals results in a reduction in the power of the techniques chosen to identify a significant hemodynamic event [4, 9, 21, 22, and 24]. For example, in a functional map given by correlation analysis, noises will lead to a decrease in the correlation as well as power of detection.

For our purposes, noises can be classified into two categories: (1) structured noises (e.g., respiration, cardiac and head movement) and (2) unstructured noises (e.g., shot noise and white noise). Much work has been done to reduce the contribution of the noise sources to the OI signal: (1) In frequency case: Because some structured noises such as 0.1Hz V-signal, head movement have the comparable time scale with the neural response signal, their spectrums distributions are heavily overlapped in low-frequency and so neither high-pass nor bass-pass [2, 3] filters can separate them in frequency effectively. (2)In spatial case: The major source of variability in the OI signal is the 0.1Hz oscillation which is present in both parenchyma and blood vessels and may be modulated by local neural activities. The signal is neither spatially nor temporally homogeneous [14-16, 18, and 23] and its spatial distribution overlaps with the activation map, so this pervasive structured noise can not be separated and removed by spatial component analysis (e.g., PCA, ICA which assume that sources are not, or at least not heavily, spatially overlapped) without influence the power of detection. (3) In temporal case: Some advances have been achieved in the area of modeling physiological noise sources by component analysis [1, 6, 11, and 23], such as tICA, PCA, and the general linear model [9, 15]. TICA can find the underlying components very well but there is also a significant risk of failure because different results may be produced in each run on identical data. PCA performs moderately in temporal analysis [6]. Mayhew and Hu [15] have applied the general linear model technique to extract V-signals by simulating the V-signals by sine waves with prior estimated frequency and phase, but one can not precisely estimated the frequency and phase, and what is more, this method can not model other structured noises without further assumptions.

In this paper, a novel technique is proposed to reduce the OI structured noises. Canonical correlation analysis (CCA) [7, 19] is applied to separate the underlying structured sources from which the neural response signal is picked out by the correlation analysis. The structured noises are then eliminated from the original data.

II. THEORY

One significant characteristic of structured noises is their high autocorrelation comparing to unstructured noises [4, 6, 7, 10-12, and 17]. When independent structured noises and the unstructured noises are linearly mixed, the mixtures are less autocorrelated than the original sources [7, 19]. So the set of uncorrelated signals with the largest autocorrelation can be

This work is supported by the Natural Science Foundation of China (60771062, 60835005) and the National Basic Research Program of China (2007CB311001).

Proc. 9th IEEE Int. Conf. on Cognitive Informatics (ICCI'10)
F. Sun, Y. Wang, J. Lu, B. Zhang, W. Kinsner & L.A. Zadeh (Eds.)
978-1-4244-8040-1/10/$26.00 ©2010 IEEE

assumed to be overcome underlying structured sources. This set of signals can be found by the technique of canonical correlation analysis which has been clearly described by Friman [7]. Refer to Appendix for further background.

In this paper, the resolution of images is denoted as $M \times N$ and the timeseries of pixels at the location (m,n) in the image is denoted as $x_{m,n}(t)$ whose length is denoted as T. It is assumed that each timeseries is a linear mixture of L uncorrelated underlying sources $s_i(t)$ ($i = 1,\cdots,L$), that is

$$x_{m,n}(t) = \sum_{i=1}^{L} w_{m,n,i} s_i(t) \quad (1)$$

Because there are much more mixtures than there are samples of each mixture, overcoming the underlying sources is an ill-posed problem. Singular value decomposition (SVD) is used to generate L-dimensional representation for the original data set. Let $\tilde{s}_i(t)$ ($i = 1,\cdots,L$; $t = 1,\cdots,T$) denote the components given by CCA in the L-dimensional subspace. In general, not all the L components given by CCA are structured sources and so a measurement is required to determine which components of the decomposition can be considered a structured one. In this paper, the white noise (WN) [6] criterion is applied to pick out the structured components from others. The WN criterion is met if the mean power across all frequency bins of the power spectrum was greater than the standard deviation of the power across all those frequency bins. The number of the components which pass the WN criterion is denotes as $\tilde{L}$.

The ideal neural response signal is then used to correlate with $\tilde{s}_i(t)$, and the component with the largest correlation is assumed to be the overcome neural response signal denoted as $\tilde{s}_{response}(t)$. The subspace spanned by the other structured components is assumed to be the physiological noises subspace and the energy of original data in this subspace is eliminated in the following way:

$$\overline{x}_{m,n} = x_{m,n} - \sum_{i=1,\tilde{s}_i \neq \tilde{s}_{response}}^{\tilde{L}} x_{m,n} \tilde{s}_i^T \tilde{s}_i \quad (2)$$

The remaining "white noise" in $\overline{x}_{m,n}$ is reduced by a low-pass filter with 7 Hz stopband edge frequency. In some statistical methods used to detect the activated pixels, such as general linear model, residuals are needed to preserve the degrees of freedom for error variance estimation, in those cases, the high-frequency noises can be hold and the autocorrelation of the unstructured noises can be used to estimated the decorrelating or whitening matrix prior to further analysis.

Because $\overline{x}_{m,n}$ contains no structured noises, it can be expected that an improved result will be given by the general techniques such as correlation analysis, first frame analysis, sICA, tICA and the general linear model etc., which are usually applied to detect the neural response signal. In this paper, the correlation analysis technique is used to demonstrate the impact of our procedure on noise reduction.

III. SIMULATION

Simulated data is generated to test the validity of the procedure proposed. A 450-frames image sequence is captured at 15 Hz from the cortex of a SD rat in the absence of any form stimulations. A 60×60 child window is further applied to the data set to pick out hindpaw (HP) area. The simulated neural response signal is added to the timeseries of 800 pixels picked out randomly in every run in the child area. The SNR is defined as the ratio between standard deviation of the neural response signal to the pixels' mean standard deviation in this paper. The correlation analysis is exploited to detect the activated pixels. When the correlation is larger than 0.8, the corresponding pixel is assumed to be activated.

The SNR varies from 1.0 to 3.5 with a step length of 0.1. Correlation analysis is applied to the original and the noise-reduced simulated data set respectively. The experiment is repeated 200 times and the mean true positive rates under different SNR are shown in Fig.1. The false positive rates with and without noise reduction under different SNR are all zero when the threshold of correlation is 0.8. As can be seen from the figure, the procedure has improved true positive rates significantly without raising the false positive rates. When the SNR is in the range 1.0 to 1.5，the mean true positive rate without noise reduction is 8.2% which means that detection is almost infeasible, while with noise reduction, the mean true positive rate in that range rises to 63.7% improved about eight times in average. With the noise reduction, the true positive rate is almost 100% when SNR is over 1.5, while the true positive rate will not reach 100% until SNR is over 3.5 if the noise reduction is not done. The true and false positive rates under different correlation thresholds, when SNR is 1.0, 1.4, 1.8 respectively, are illuminated in Fig. 2. It can be seen from the figure that when the correlation threshold is over 0.6, the true positive rates with noise reduction are much higher than those without noise reduction. This hints that correlations of the activated pixels have risen significantly and the activated pixels are more clustered and easier to be detected after the noise reduction. A relatively high correlation threshold can be applied to noise-reduced data to give a more reliable result.

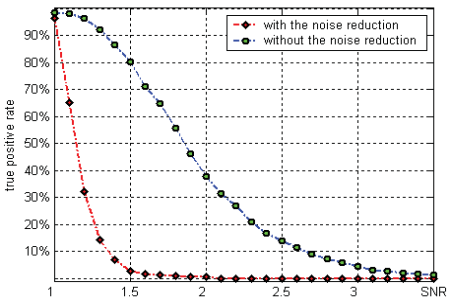

Figure 1. The true positive rates under different SNR with and without noise reduction.

Given as an example, the overcome underlying sources which pass the WN measure when the SNR is 1.2 are shown in Fig.3. They are ranked in descent by their autocorrelation. The first one is the simulated neural response signal and the second one is the 0.1Hz vasomotion signal. The histograms of the correlations of inactivated and activated pixels are shown in

Fig. 4. The Fig. 4-a/c are the histograms of correlations of inactivated/activated pixels with the noise reduction, and the Fig. 4-b/d are the histograms of inactivated/activated pixels without the noise reduction. Comparing the histograms before and after the noise reduction, it can be found that the correlations of activated pixels move toward 1.0 after the noise reduction. The mean correlation of activated pixels rises from 0.5056 to 0.8229 while the standard deviation of the correlations descends from 0.5056 to 0.0718 decreased about eight times which means that the activated pixels are more clustered after the noise reduction. The mean correlation of inactivated pixels descends from -0.1295 to -0.2740 and the standard deviation rises from 0.1651 to 0.2462. The shift of the correlation distribution of inactivated pixels is perhaps due to the inaccuracies in data reconstruction. The assumption that all the underlying sources are all independent to each other may not be strictly met in the real application. The distance between centers of two classes of pixels' correlation rises from 0.64 to 1.1 which means the activated pixels are more distinct from the inactivated ones and so easier to be separated.

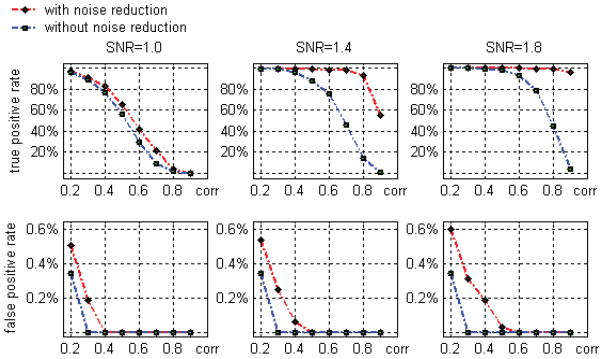

Figure 2. The true and false positive rates under different correlation threshold when SNR is 1.0, 1.4, 1.8 respectively.

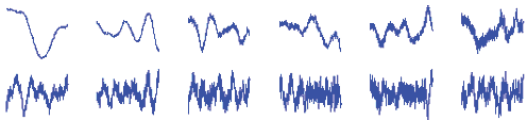

Figure 3. The components given by CCA which passed the WN criterion when SNR is 1.2. The components are ranked in descent by their autocorrelation. The first one is the overcome neural signal response and the second one is the 0.1Hz vasomotion signal.

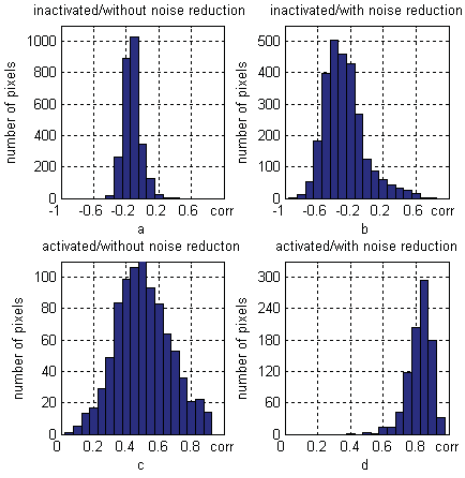

Figure 4. The histograms are as following: 4-a/b are the histograms of inactivated/activated voxels's correlations without the noise reduction, 4-c/d are the histograms of inactivated/activated voxels's correlations with the noise reduction.

IV. OI DATA PROCESSING

The procedure has been applied to five sets of the OI data collected from rat's HP areas with sciatic nerve stimulation.

A. Animal preparation and data collection

Functional intrinsic optical imaging signals were collected from five rats' HP areas. The rats weight between 200 and 350g and were kept in a 12-h dark/light cycle environment at a temperature of 22℃. The animals were anesthetized with urethane (1g/kg) and atropine was also administered (0.24mg/kg) to reduce mucous secretions. This area of cortex as known is a proper model for investigating the coupling of neuronal activity, the perfusion-related and the metabolic responses.

A dental drill was used to thin the skull over the interested cortical area uniformly until the arterioles and veins could be visualized in the field of the view of the detector. Silicon oil was applied to the skull in order to increase the translucency of the skull in the duration of the imaging period. Optical imaging series were collected by a slow-scan digital CCD working at 15Hz. The CCD has a 12 bit analog-to-digital converter. The duration of each trial is 30 seconds and altogether 450-frames of images were collected in each trial. The cortex was illuminated at 560 10 nm using a stabilized light source. An electrical stimulation (5Hz, 5V) of median nerve at the hindpaw was applied to rats from the beginning of 10th second to the end of 11th second in all trials.

B. Data processing

The proposed noise reduction procedure is applied to the five data sets and then correlation analysis is exploited to detect the activated pixels. Two activation maps with and without the noise reduction are shown as an example in Fig.5. The Fig.5-a /c are maps without noise reduction and the corresponding noise-reduced activation maps are shown in Fig.5-b/d. More detailed spatial architectures are revealed in Fig. 5-b/d than in Fig.5-a/c. It can be found in Fig.5-b/d that the most activated pixels lie at arterial areas which can not be discerned in Fig.5-a/c. This is consistent with the finding that the origin of intrinsic OI is more arterial [5].

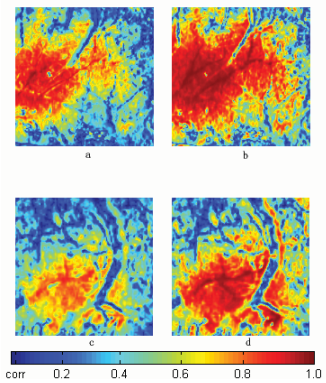

Figure 5. The activation maps with and without noise reduction: Fig. 5-a/c are activation maps given by correlation analysis without noise reduction from two data sets and Fig. 5-b/d are corresponding noise-reduced activation maps from the same data sets.

V. Discussion

CCA is an effective technique for discerning the underlying structured sources. Followed by deletion of undesirable components and the reconstruction of the data, CCA can be used successfully to reduce the structured noises. In the OI data, the physiological noises are the dominating factors [4, 6, 10, and 22] which are all structured noises and can be extracted by CCA stably and robustly. PCA and tICA can also be exploited to achieve this task. Some researchers [7] have investigated effects of PCA and tICA on extracting the underlying components comparing to CCA. In their conclusion, PCA is less efficient than tICA and CCA is almost same efficient as tICA. But tICA has a serious shortcoming which cumbers its application. In general, when applied to the identical data set, tICA may give quite different results in different run, so a supervisor is required to evaluate the result. It is obvious that tICA is not a proper choice for an unsupervised noise reduction procedure. CCA always gives the identical result in each run and needs much less computing time than tICA. Furthermore, CCA is less influenced by the high-frequency noises than the tICA and the resulting components are smoother than those given by tICA. The CCA tends to be more robust than tICA with respect to the low sample size in the temporal analysis and the reason may be that measuring autocorrelation does not require as many samples as measuring non-Gaussianity [7].

In CCA, the underlying sources are assumed to be independent as in the tICA, so before we draw any conclusion, how well the assumptions apply should be considered. In temporal case the assumption that timeseries of each pixels contains several independent underlying sources (e.g., low-frequency vasomotions, stimulus-induced responses and drifts) can be accepted in OI data. The assumption of independence may be violated because of the relatively little number of the samples, the correlation between two finite length observations of the underlying independent sources may significantly differ from zero which will lead to false results, but this will have little possibility if the length of observations is long enough and the sample frequency is relatively high. In general, the sample frequency of OI technique is over 10Hz and the data length is over 200 frames which makes the risk that correlation between observations of two hypothetic independent sources differs significantly from zero small.

Some papers [13-16, 20] have pointed that the 0.1Hz vasomotion is a leading noise source in the OI data, the amplitude of 0.1Hz "noise" is at least an order of magnitude greater than the differential mapping signals used to reveal functional architecture [14-16]. The 0.1Hz signal and the stimulus-induced signal heavily overlay in frequency and they almost have the same temporal scale. In some cases, the 0.1Hz signal would strongly modulate the stimulus-induced signal and make it difficult to detect the activated pixels. Some researchers [15] have tried to eliminate 0.1Hz noise by the general linear model technique which simulates the V-signal by sine wave with different frequency and phase. However, the researchers can not precisely estimate the frequency and phase of V-signal, and what is more, the frequency and the phase may all drift from the baseline during the data collection. CCA is a data-driven method which need not model the signal in advance and it extracts the underlying structured sources by their high autocorrelation which is a distinct characteristic for 0.1Hz signal. In our experiments, the 0.1Hz signal is stably extracted in all trials. So CCA is also a valuable technique for 0.1Hz investigation.

VI. Conclusions

A reliable, stable and less time consuming procedure which aims to detect and eliminate the structured noises is proposed in this paper. The Monte Carlo simulation and the OI data processing indicate that our procedure is a valuable additional choice to the family of the preprocessing techniques used to improve the power of the detection. Without the influence of the structured noises such as 0.1Hz signal, low-frequency drifts etc., the general analysis methods applied to OI data can give an improved result. The procedure can also be applied to fMRI and EEG data.

Appendix: Canonical Correlation Analysis

Let $X(t)=\{x_1(t),\cdots,x_n(t)\}$ be denoted as the original data matrix with n mixtures and $t=1,\cdots,N$ samples of each mixture. Denote $Y(t)$ a temporally k-step delayed version of the $X(t)$. The mean of each row from the matrices $X(t)$ and $Y(t)$ are subtracted firstly. Denote the component that has the most autocorrelation as: $z_1(t)=w_{11}x_1(t)+\cdots+w_{1n}x_n(t)=w_1^T\times X$, whose k-step autocorrelation can be written as

$$\begin{aligned}\rho_k &= \frac{E\{z_1(t).z_1(t-k)\}}{\sqrt{\mathrm{var}\{z_1(t)\}\cdot\mathrm{var}\{z_1(t-k)\}}} \\ &= \frac{E\{\alpha^T x(t)\cdot(\alpha^T x(t-k))^T\}}{\sqrt{\{E[\alpha^T x(t)\cdot x^T(t)\alpha]E[\alpha^T x(t-k)\cdot x^T(t-k)\alpha\}}} \\ &= \frac{\alpha^T C_{x(t)x(t-k)}\alpha}{\left\{\sqrt{\alpha^T C_{x(t)x(t)}\alpha}\sqrt{\alpha^T C_{x(t-k)x(t-k)}\alpha}\right\}}\end{aligned} \tag{3}$$

where ρ_k reaches the maximum when the vector $w_1=\{w_{11},\cdots,w_{1n}\}$ satisfy the following equation:

$$C^{-1}_{x(t)x(t)}C_{x(t)x(t-k)}C^{-1}_{x(t-k)x(t-k)}C_{x(t-k)x(t)}w_1=\rho_k{}^2 w_1 \tag{4}$$

It is obvious that ρ_1 and w_1 are the eigenvalue and the corresponding eigenvector of the matrix $C^{-1}_{x(t)x(t)}C_{x(t)x(t-k)}C^{-1}_{x(t-k)x(t-k)}C_{x(t-k)x(t)}$ respectively. Following the same way, we can get the other components and their autocorrelation one by one. The within- and between-set covariance matrices in equation (2) are estimated as following:

$$\begin{aligned}
\tilde{C}_{x(t)x(t)} &= \frac{1}{T}\sum_{t=1}^{T} x(t)x(t)^T \\
\tilde{C}_{x(t-k)x(t-k)} &= \frac{1}{T}\sum_{t=1}^{T} x(t-1)x(t-k)^T \\
\tilde{C}_{x(t)x(t-k)} &= \frac{1}{T}\sum_{t=1}^{T} x(t)x(t-k)^T \\
\tilde{C}_{x(t-k)x(t)} &= \frac{1}{T}\sum_{t=1}^{T} x(t-k)x(t)^T
\end{aligned} \tag{5}$$

Insert the estimated covariance matrices into equation (2) and solve the eigenvalue problem to find the unmixing matrices $w = \{w_1, \cdots, w_n\}^T$ resulting in the estimations $\hat{z}(t)$ of the underlying sources $z(t)$. In our paper the delay is denoted one frame, that is $Y(t) = X(t-1)$.

In the real application, *n*, the number of mixtures is much larger than the number of the underlying independent sources, so the SVD or the PCA is required to reduce the dimensionality to a proper value. In this paper SVD is exploited.

REFERENCES

[1] A. H. Andersen, D. M. Gash, and M. J. Avision. Principal component analysis of the dynamic response measured by fMRI: A generalized linear systems framework. Magn. Reson. Imaging, vol. 17, pp.795-815, 1999.

[2] B. Biswal, E. A. DeYoe, and J. S. Hyde. Reduction of physiological fluctuations in fMRI using digital filters. Magn. Reson. Med., vol. 35, pp.107-113, 1996.

[3] T. Bonhoeffer, and A. Grinvald. Optical imaging based on intrinsic signals: the methodology. In Brain Mapping: The methods (A. Toga and J. C. Maziotta, Eds.), Academic Press, San Diego, CA, pp.55-97, 1996.

[4] E. D. Bullmore, C. Long, J. Suckling, J. Fadili, G. Calvert, F. Zelaya, A. Carpenter, and M. Brammer. Colored noise and computational inference in neurophysiological(fMRI) time series analysis: resampling methods in time and wavelet domains. Human Brain Mapping, vol. 12, pp.61-78, 2001.

[5] A. F. Cannestra, N. Pouratian, S. Y. Bookheimer, N. A. Martin, D. P. Becker, and A. W. Toga. Temporal spatial differences observed by functional MRI and human intraoperative optical imaging. Cerebral cortex, vol. 11, pp.773-782, 2001.

[6] G. T. Christopher, A. H. Richard, and S. Ravi. Noise reduction in BOLD-based fMRI using component analysis. NeuroImage, vol. 17, pp.1521-1537, 2002.

[7] O. Friman, M. Borga, P. Lundberg, and H. Knutsson. Exploratory fMRI analysis by autocorrelation maximization. NeuroImage, vol. 16, pp.454-464, 2002.

[8] R. D. Frostig, E. E. Lieke, D. Ts'o, and A. Grinvald. Cortical functional architecture and local coupling between neuronal activity and the m microcirculation revealed by in vivo high-resolution optical imaging of intrinsic signals. Proc. Natl. Acad. Sci. USA, vol. 87, pp.6082-6086, 1990.

[9] K. J. Friston, A. P. Holmes, J. B. Poline, C. Frith, R. S. J. Frackowiak. Statistical parametric maps in functional imaging: A general linear approach, Human Brain Mapping, vol. 2, pp.189-210, 1995.

[10] K. J. Frison, O. Josephs, E. Zarahn, A. P. Holmes, S. Rouquette, and J. B. Poline. To smooth or not smooth? NeuroImage, vol. 12, pp.196-208, 2000.

[11] V. Kiviniemi, J. H. Kantola, Independent component analysis of the nondeterministic fMRI signal sources, NeuroImage, vol. 19, no.2, pp.253-260, 2003.

[12] G. Kruger, and G. H. Glover. Physiological noise in oxygenation-sensitive magnetic resonance imaging. Magn. Reson. Med, vol. 46, pp.631-637, 2001.

[13] T. H. Le, and X. Hu. Retrospective estimation and correction of physiological artifacts in fMRI by direct extraction of physiological activity from MR data. Magn. Reson. Med., vol. 35, pp.290-298, 1996.

[14] J. E. W. Mayhew, S. Askew, Y. Zheng, J. Porrill, G. W. M Westby, P. Oedgrave, D. M. Rector, and R. M. Happer. Cerebral vasomotion: A 0.1-Hz oscillation in reflected light imaging of the neural activity. NeuroImage, vol. 4, pp.183-193, 1996.

[15] J. E. W. Mayhew, D. W. Hu, Y. Zheng. S. Askew, Y. Q. Hou, J. Berwick, P. J. Coffey, and N. Brown. An evaluation of linear model analysis techniques for processing images of micro-circulation activity. NeuroImage, vol. 7, no. 1, pp.49-71, 1998.

[16] J. E. W. Mayhew, S. Askew, Y. Zheng, J. Porrill, G. W. M. Westby, P. Redgrave, D. M. Rector, and R. M. Harper.. Cerebral vasomotion: 0.1Hz oscillation in imaging of neural activity. Soc. Neurosci. Abstr, vol. 21, pp.656-659, 1995.

[17] J. M. Martin, V. Vijay, H. Scott and M. Gregory. Deterministic and stochastic features if fMRI data: implications for analysis of event-related experiments. Journal of Neuroscience Methods, vol. 118, pp.103-113, 2002.

[18] M. J. Mckeon, S. Makeig, G. G. Brown, T. P. Jung, S. S. Kindermann, and T. J. Sejnowski. Analysis of fMRI data by blind separation into independent spatial components. Human Brain Mapping, vol. 6, pp.368-372, 1998.

[19] L. Molgedey, H. Schuster, Separation of an independent signals using time delayed Correlations Phys. Rev. Lett., vol. 72, pp.3634-3636, 1994.

[20] Y. Morita, E. Bouskela, and J. E. Hardebo. Vasomotion in the rat cerebral microcirculation recorded by laser- Doppler flowmetry. Acta Physiol. Scand., vol. 146, pp.431-439, 1992.

[21] S. Ogawa, P. P. Mitra, X. Hu, and K. Ugurbil. Spatio-temporal patterns revealed in denoised fMRI data. Electroencephalogr. Clin. Neurophysiol. Suppl., vol. 47, pp.5-14, 1996.

[22] L. P. Patrick, M. W. Robert. Effect of temporal autocorrelation due to physiological noise and stimulus paradigm on voxel-level false-positive rates in fMRI. Human Brain Mapping, vol. 6, no. 4, pp.239-249, 1998.

[23] M. Stetter, I. Schiebl, F. Sengpiel, M. Hubener, T. Bonhoeffer. and K. Obermayer. Principal component analysis and blind separation of the sources for optical imaging of intrinsic signals. NeuroImage, vol. 11, pp.482-490, 2000.

[24] M. W. Woolrich, B. D. Ripley, M. Brady, and S. M. Smith. Temporal autocorrelation in univariate linear modeling of fMRI data. NeuroImage, vol. 14, pp.1370-1386, 2001.